Supporting Information

O_2-Cu/ZIF-8@Ce6/ZIF-8@F127 Composite as a Tumor Microenvironment-Responsive Nanoplatform with Enhanced Photo / Chemo-Dynamic Antitumor Efficacy

Zhongxi Xie, ‡,§ Shuang Liang,‡,§, Xuechao Cai,§ Binbin Ding,‡,§, Shanshan Huang, ‡ Zhiyao Hou, ‡ Ping ′an Ma, ‡ Ziyong Cheng*‡,§ and Jun Lin* ‡,§

‡ State Key Laboratory of Rare Earth Resource Utilization, Changchun Institute of Applied Chemistry, Chinese Academy of Sciences, Changchun 130022, PR China

§ University of Science and Technology of China, No. 96, JinZhai Road, Baohe District, Hefei, Anhui 230026, P. R. China.

* Corresponding author.
E-mail address: zycheng@ciac.ac.cn; jlin@ciac.ac.cn

List of Abbreviations in This Study[a]

Full Name	Abbreviations	Full Name	Abbreviations
Chemodynamic Therapy	CDT	O_2-Cu/ZIF-8@Ce6/ZIF-8 Nanocomposites	OCZC
Chlorin e6	Ce6	O_2-Cu/ZIF-8@Ce6/ZIF-8@F127 Nanocomposites	OCZCF
Cu/ZIF-8@Ce6/ZIF-8@F127 Nanocomposites	CZCF	Photodynamic Therapy	PDT
Cu-doped ZIF-8	Cu/ZIF-8	Reactive Oxygen Species	ROS
Enhanced Permeability and Retention	EPR	Tumor Microenvironment	TME
Glutathione	GSH	Zeolitic Imidazolate Frameworks	ZIFs
Metal-organic Frameworks	MOFs	ZIF-8@Ce6/ZIF-8@F127 Nanocomposites	ZCF

[a] Sort by the initials of the full name.

Tables and Figures:

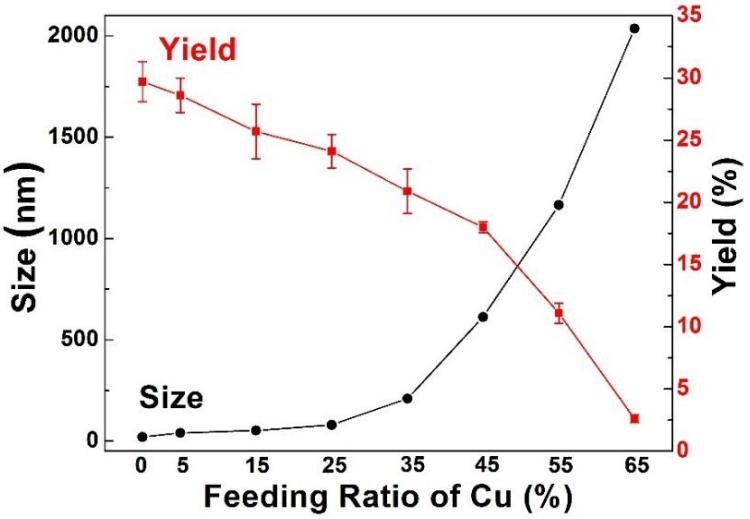

Figure S1. Plots of the average diameter and yield of Cu/ZIF-8 with different amount of Cu (%). The particle size was given by dynamic light scattering (DLS) analysis. The product yield was calculated from inductively coupled plasma (ICP) results.

Table S1. The average diameter of Cu/ZIF-8 with different amount of Cu.

C_{Cu}[a] (%)	C_{Cu}[b] (%)	Particle Size (nm)	PdI[c]
0	0	20	0.07
5	1.5	40	0.52
15	3.8	52.1	0.46
25	5.9	79.7	0.41
35	8.3	209.8	0.49
45	11.5	612.3	0.28
55	13.4	1165.5	0.22
65	14.2	2036.8	0.37

[a] The feeding ratio of $Cu(NO_3)_2$. [b] The real molar content of Cu given by ICP. [c] Polydispersity index defined as PdI = σ/m, in which d - dispersity, σ - standard deviation from mean value, m -

mean size of nanoparticles.

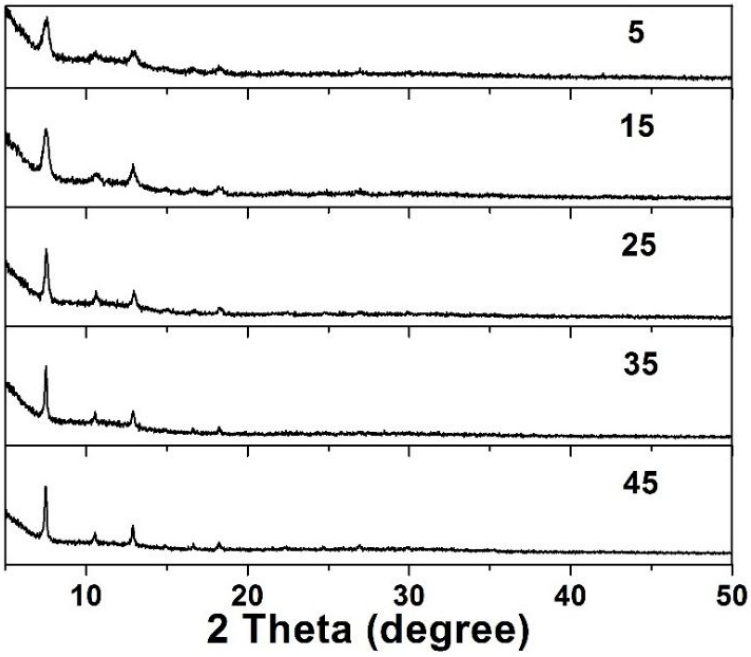

Figure S2. Powder X-ray diffraction (PXRD) patterns of Cu/ZIF-8 with different amount of Cu (%). As the Cu doping percentage increasing, a slight decrease in the full-width at half-maximum of the (011) peak intensity ($2\theta = 7.35°$) is observed, which suggests the increased particle size.

Table S2. Particle size, polydispersity index (PdI) and Zeta potential of Cu/ZIF-8, OCZC, and OCZCF, respectively. All results were measured by DLS analysis.

	Cu/ZIF-8	**OCZC**	**OCZCF**
Particle Size (nm)	79.7	86.1	97.8
PdI	0.41	0.59	0.66
Zeta Potential (mV)	7.88	6.81	0.137

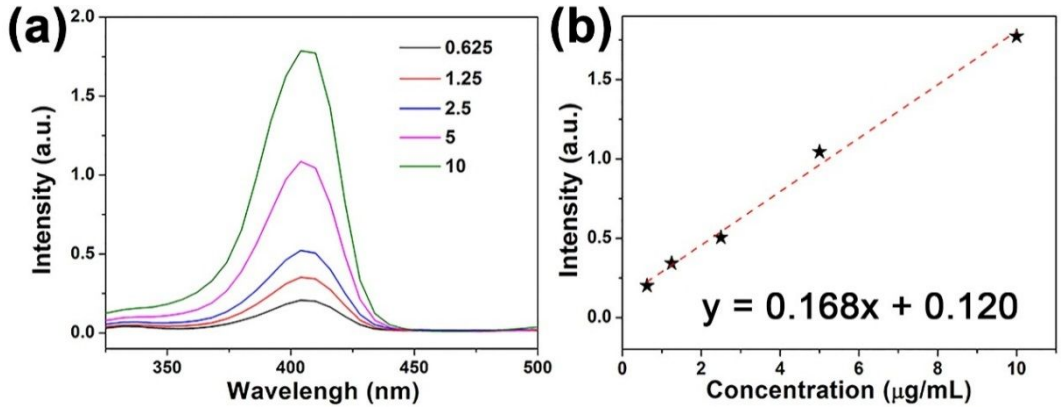

Figure S3. (a) Standard UV-vis absorption curve of Ce6 dispersed in EtOH. (b) The peak intensity of Ce6 at 410 nm shows a linear relationship with the Ce6 concentration: Y = 0.168X + 0.120, in which X - the concentration of Ce6, Y - The peak intensity of Ce6 at 410 nm.

Table S3. A comparison of the BET surface (S_{BET}), microporous volume (V_{micro}), and pore size for ZIF-8, Cu/ZIF, and CZC nanoparticles, respectively.

	S_{BET} (m^2/g)	V_{micro} (cc/g)	Pore Size (nm)
ZIF-8	2240	1.95	0.63
Cu/ZIF	2177	1.67	0.63
CZC	2122	1.25	0.61

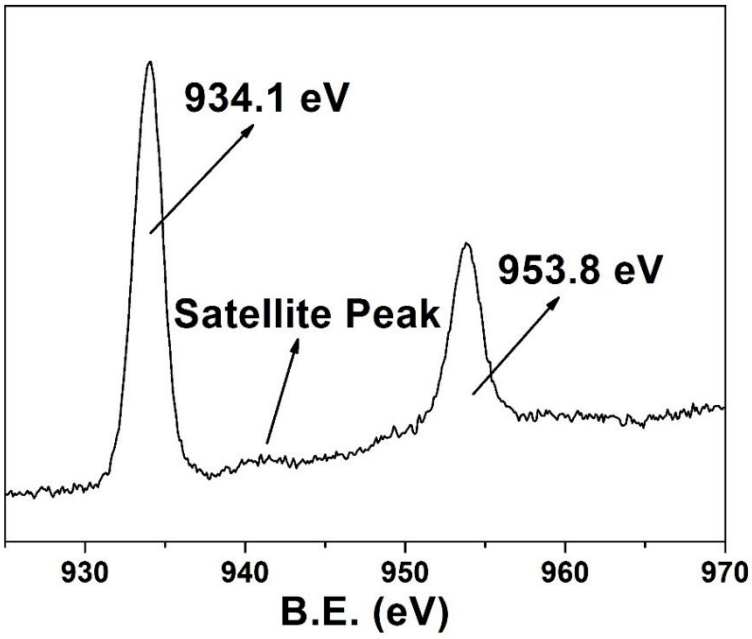

Figure S4. High-resolution XPS Cu(2p*)* spectra of OCZCF. The peaks at 934.1 and 953.8 eV are assigned to the Cu($2p_{3/2}$) and Cu($2p_{1/2}$) of Cu^{2+}, respectively.

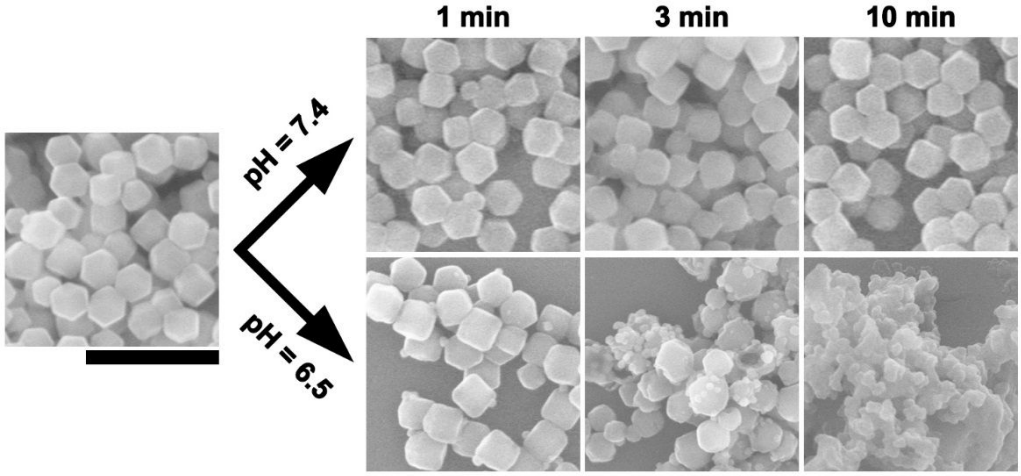

Figure S5. SEM images of OCZCF after immersed in PBS solution (pH = 6.5 and 7.4) for different time intervals. Scale bar indicates 300 nm. The crystal decomposed after soaking in PBS buffer with pH = 6.5 for 10 min.

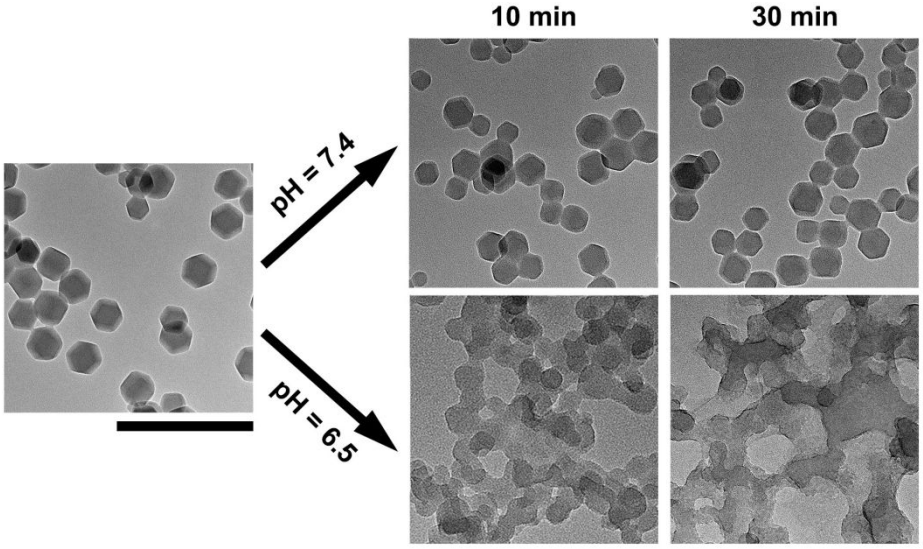

Figure S6. TEM images of OCZCF after immersed in PBS solution (pH = 6.5 and 7.4) for different time intervals. Scale bar indicates 300 nm. The crystal started decomposing after soaking in PBS buffer with pH = 6.5 for 10 min and decomposed thoroughly at 30 min.

Table S4. ICP results of the average amount of Cu (n = 3) released by OCZCF (25mg) after soaking in PBS solutions (10 mL, pH = 6.5 and 7.4).

Time (min)		**1**	**2**	**3**	**4**	**5**
pH = 7.4	**C_{Cu} (ppm)**	18.9	3.32	6.07	6.94	2.30
	P[a] (%)	4.2	0.74	1.35	1.54	0.51
pH = 6.5	**C_{Cu} (ppm)**	229.62	121.90	24.85	7.42	4.00
	P[a] (%)	51.03	27.09	5.52	1.65	0.89

[a] The released percentage of Cu

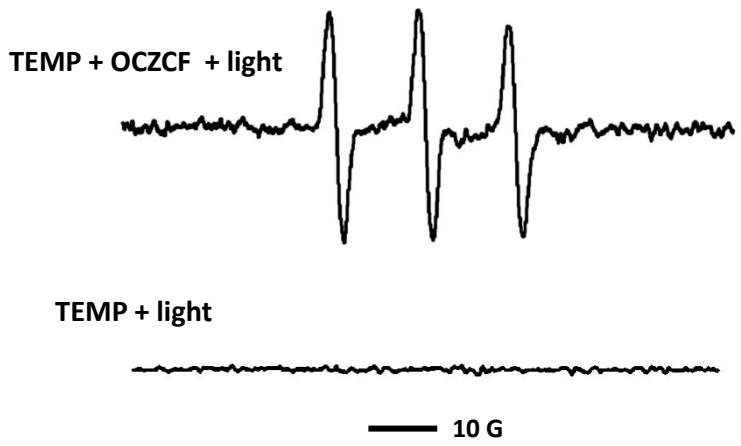

Figure S7. ESR spectra under 650 nm laser irradiation (50 mW/cm^2, 10 min) with and without OCZCF in the presence of TEMP.

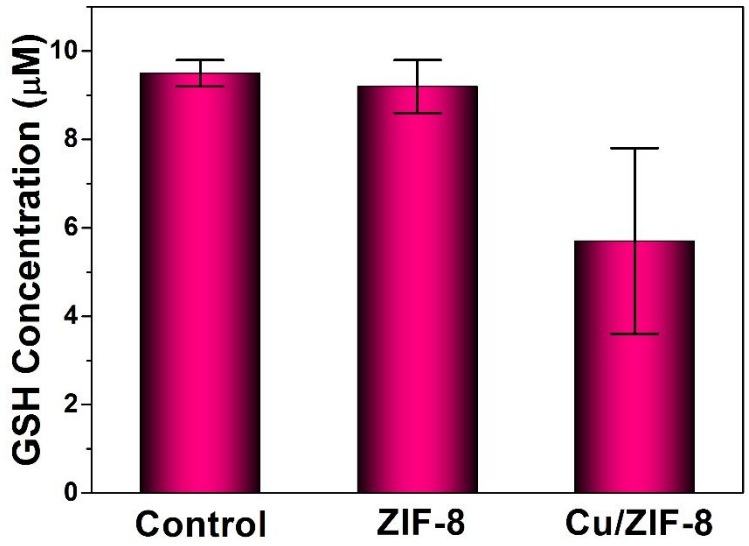

Figure S8. The GSH concentration when incubated with PBS (control group), ZIF-8 and Cu/ZIF-8 in acidic PBS buffer (pH = 6.5), respectively.

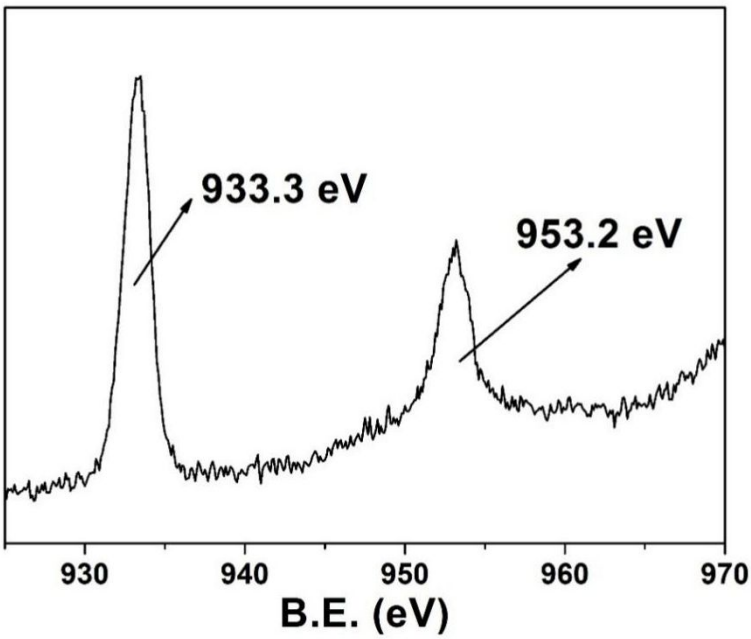

Figure S9. High-resolution XPS Cu(2p*)* spectra of OCZCF after incubating with GSH. Compared with OCZCF, the binding energy shifted from 934.1 and 953.8 eV of Cu^{2+} to 933.3 and 953.2 eV, respectively. Besides, the satellite peak at around 942.3 eV dissappears, indicating the existance of Cu^{+}.

Figure S10. ESR spectra with and without OCZCF in the presence of DMPO.

Table S5. Uptake of OCZCF at different time points in both normal and cancer cells by ICP-MS

	0 h	1 h	2 h	4 h	6 h
L929 cells	12.160 ppm	178.9 ppm	160.7 ppm	177.5 ppm	248.0 ppm
4T1 cells	11.650 ppm	196.1ppm	240.4 ppm	244.5 ppm	226.8 ppm

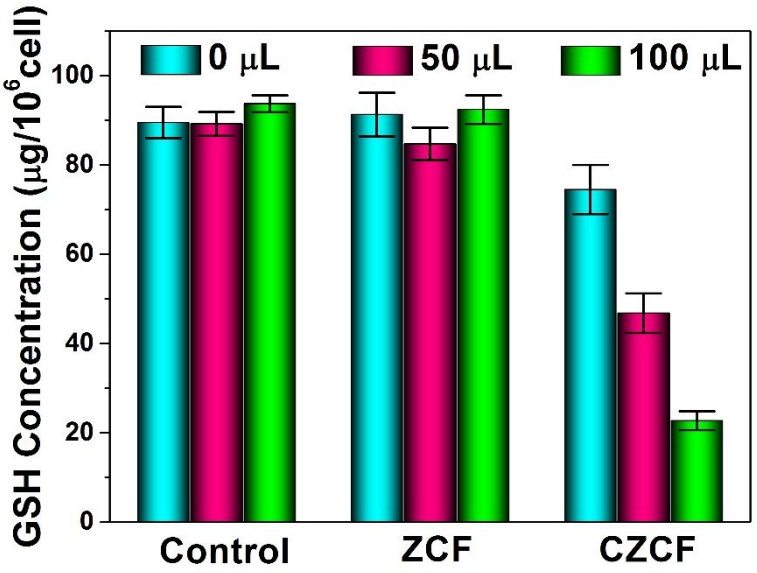

Figure S11. Mass of the intracellular GSH in 4T1 cells treated with PBS, ZCF and CZCF for 12 h, respectively. The sharp decrease of GSH concentration in CZCF group demonstrates the GSH consumption by copper-containing CZCF component in tumor cells.

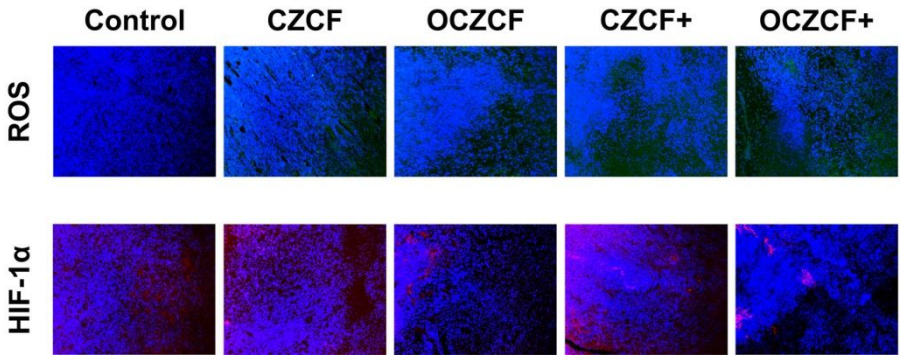

Figure S12. Micrograph images of tumor slices with ROS and HIF-1α fluorescence staining, respectively.

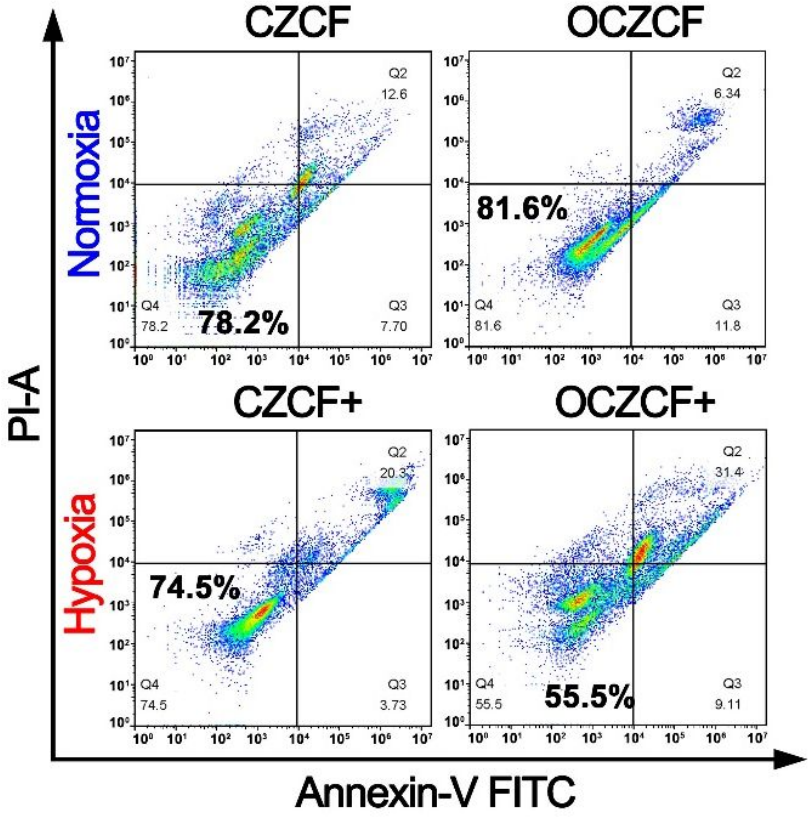

Figure S13. Flow cytometry analysis of 4T1 cells incubated with CZCF or OCZCF under different condition. The concentration of nanodrug was 20 μg mL^{-1}. 650 nm laser irradiation at a power density of 50 mW cm^{-2} for 5 min. The live and dead cells were stained via annexin V-FITC and PI staining kit. Under hypoxia, OCZCF+

exhibits higher lethality than CZCF+ treatment, suggesting the importance of overcoming hypoxia for enhanced PDT and CDT.

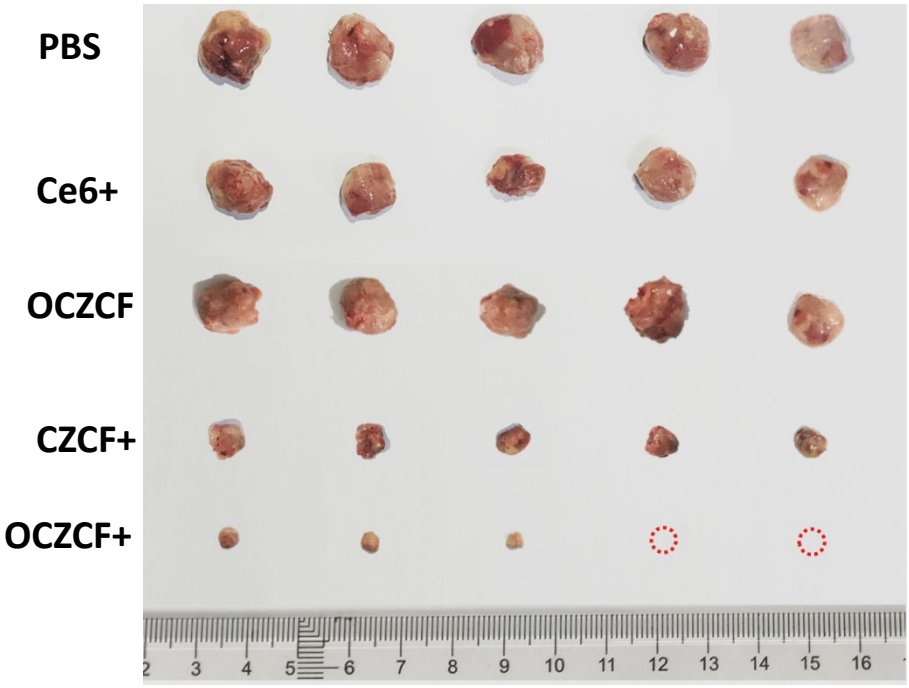

Figure S14. Photograph of tumors collected from Balb/c mice treated with different materials at the end of the treatment. The blue circle indicates the complete retrogression of tumor after treating with OCZCF+.

Table S6. Blood biochemical indexes of mice after treated with PBS, Ce6+, OCZCF, CZCF+, and OCZCF+, respectively. (heart function: creatine kinase - CK2; kidney function: urea - UREA, creatinine; liver function: alanine transaminase - ALTL, aspartate transaminase - AST). **p < 0.01, *p < 0.05. These results demonstrate that OCZCF does not cause serious anaphylaxis.

Bio-Index	Control		Ce6+		OCZCF	
	Average	SD	Average	SD	Average	SD
CK2	1449.33	66.16	1938(*)	186.59	1827.67(*)	175.31
ALTL	32.75	2.56	41.77(*)	5.38	37.46	10.48
AST	154.44	16.95	166.89	25.04	169.33	20.43
UREA	5.89	1.18	7.58	2.01	9.06	3.62
CREA	4.77	0.67	6.95	1.30	6.07	1.39

Bio-Index	CZCF+		OCZCF+	
	Average	SD	Average	SD
CK2	1712.33	342.59	2084.33	271.80
ALTL	41.39	7.40	42.46(**)	3.20
AST	208.33(*)	4.92	160.33	22.57
UREA	9	2.10	10.52	1.41
CREA	7.84	2.01	9.38(*)	0.46

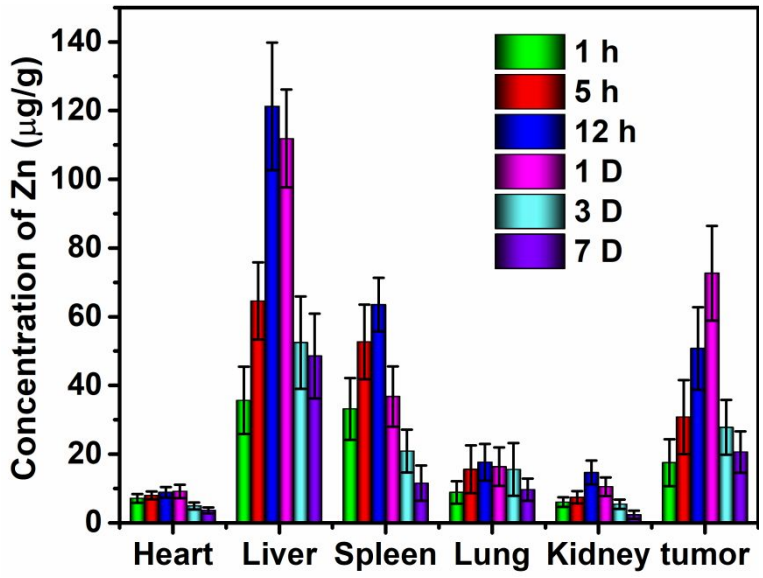

Figure S15. The in vivo biodistribution of Zn after i.v. injection with OCZCF at different time